

Size Limit of Defect Formation in Pyramidal Pt Nanocontacts

V. Rodrigues,^{1,*} F. Sato,¹ D. S. Galvão,¹ and D. Ugarte^{1,2}

¹*Instituto de Física “Gleb Wataghin,” Universidade Estadual de Campinas, Unicamp, C.P. 6165, 13083-970, Campinas, São Paulo, Brazil*

²*Laboratório Nacional de Luz Síncrotron, C.P. 6192, 13084-971, Campinas, São Paulo, Brazil*
(Received 30 July 2007; published 19 December 2007)

We report high resolution transmission electron microscopy and *ab initio* calculation results for defect formation in sharp pyramidal Pt nanocontacts. Our results show that there is a size limit to the existence of twins (extended structural defects). These defects are always present but blocked away from the tip axes. They may act as scattering planes, influencing the electron conductance for Pt nanocontacts at room temperature and Ag/Au nanocontacts at low temperature (<150 K).

DOI: [10.1103/PhysRevLett.99.255501](https://doi.org/10.1103/PhysRevLett.99.255501)

PACS numbers: 62.25.+g, 61.72.Nn, 68.37.Lp

The structural and mechanical properties of nanometric wires represent a fundamental issue for the understanding of different phenomena such as friction, fracture, adhesion, etc. [1]. There is renewed interest in such systems motivated by the growing demand on nanotechnology miniaturization, new functionalities, and less power consuming systems. Components such as diodes [2], switches [3], and electronic mixers [4] have been built with simple molecules as active units [5]. In spite of these technological advances, important aspects on device integration (e.g., how to connect them in a stable and reproducible way) are still open issues [6,7]. In order to build functional nanodevices, electrical contacts of nanometric dimensions are needed. The contact atomic arrangement will probably determine the electronic structure and, as a consequence, the coupling between leads and the active part (for example, molecules) of the device [7–9]. In this context, it is necessary to understand the influence of lead properties in the device characteristics and also the role played by structural defects since they can compromise the device functionality and reliability [10]. Unfortunately, their fabrication and characterization are rarely possible; consequently, control and reproducibility are still very difficult, even for the simplest cases, such as the hydrogen molecule [11].

Most experimental studies of nanometric metal contacts have been based on mechanical elongation of metal nanowires. Nanocontacts (NCs) have been used with different meanings in the literature; in this Letter NC is used to describe the whole electrical lead, for example, the 7 plane atomically sharp tip from Fig. 1(c). These NCs can connect the active part of the device, as an atom or a molecule. In order to get a deeper understanding of the NC electrical properties, its mechanical and atomic structure should be better investigated. For atomic size NCs generated by mechanical stretching, we can expect that the deformation must exhibit stages where structural defects are formed to accommodate the elongation strain. It has already been reported that mechanical elongation exhibits distinct elastic strain stages, followed by sharply defined yielding,

originating from structural reorganization [1,12,13]. In this way, we cannot properly address the deformation of nanosystems using continuum-based theories; a microscopic analysis taking into account the atomic structure is necessary. The plastic deformation is associated with collective slips of entire atomic planes or order-disorder transitions [13,14]. It has been suggested that at very small scales (10 nm) dislocations should be completely suppressed because the involved stress is comparable to the intrinsic lattice strength. In analogy, a self-purification effect has been recently reported for semiconductor particles: defect formation energy increases as the nanocrystal size decreases, rendering difficult the doping of smaller systems [15,16].

In this sense some fundamental questions must be addressed. Is small perfect? Can we generate defect-free metallic NCs? Is there a size limit for defect generation? In the case of pyramidal electrical leads, size limit would represent a minimum distance from the defect to the atomically sharp apex. In this Letter we present results from dynamic high resolution transmission electron microscopy (HRTEM) experiments of the atomic arrangement of Pt NCs under mechanical deformation at room temperature.

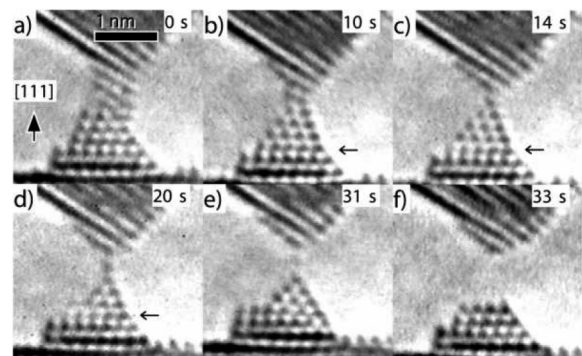


FIG. 1. Sequence of images showing the elongation and rupture of a Pt NC under tensile stress with a minor shear component (observation axis $[1\bar{1}0]$). Arrows in (b)–(d) indicate the twin position.

We have observed that there is a minimal distance to the atomically sharp tip where extended structural defects (twins) can exist; in fact, defects are always present but blocked a few atomic planes away from the sharp Pt tip. In order to quantitatively estimate the size limit where defect-free contacts can exist, we have estimated the energetics associated with the twin generation through *ab initio* calculations using the SIESTA code [17].

The atomic size metal NCs were generated *in situ* in a HRTEM (JEM 3010 URP, 300 kV, 0.17 nm point resolution, operating at LME/LNLS, Campinas, Brazil). In this methodology, the microscope electron beam is focused to generate holes in a self-supported thin metal film until neck is formed between them [18]. The NCs (1–2 nm in diameter) spontaneously become thinner due to displacements of the apexes, reach the size of a few atoms and finally break. During this process, we have no control on the direction or speed of the elongation. Real time structural evolutions were recorded using a high sensitivity TV camera (Gatan 622SC, 30 frame/s).

For the theoretical analysis we have used *ab initio* density functional theory (DFT) in the framework of the local density approximation (LDA) [17,19]. In order to warrant high precision results, we have used double-zeta basis set plus polarization functions (relativistic calculations) and norm-conserving pseudopotentials built on Troullier-Martins scheme [20]. We have also carried out generalized gradient approximation (GGA) calculations developed by Perdew, Burke, and Ernzerhof [21]. We first tested the parameters used on the SIESTA code for Pt perfect crystalline bulk structures, relaxing both cell lattice vectors and atomic positions. The obtained values are in good agreement with the experimental ones [3.924 Å and 3.875 (3.983) Å, for the experimental [22] and SIESTA LDA (GGA) values, respectively]. Once the pseudopotential reliability for Pt structures was established, we proceeded to analyze the energetics and relative stability of the structures with defects (twins). As the structures are not in their global energy minima, in order to preserve the pyramidal shape, the geometrical optimizations have to be carried out using constraints, in our case setting up an upper limit to atom displacements (0.01 Å) and forces (0.08 eV/Å).

The analyses of HRTEM images, from more than 40 experimental runs, always display Pt NCs where the first layers (counting from the tip) can be considered defect-free crystalline Pt nanoconstrictions. When aligned with the HRTEM beam, the atomic resolved micrographs allow us to observe that defects are always away from the tip. As an illustrative example, Fig. 1 shows a nanostructure where the lower apex is well aligned with the HRTEM beam, thus providing atomic and time resolved images of a pyramidal tip contact. Its axis is along the [111] crystalline direction, and it ends with only one atom. In the lower apex, the horizontal lattice periodicity is 0.24 ± 0.01 nm [Pt (111) spacing is 0.227 nm], and the angular relations confirm that the pyramid is defined by a (111) and (100) facet at left and

right, respectively. The apex vertical movement generates the NC thinning, but a small shear movement (upper apex is gliding to the right) has induced the formation of a kink on the left apex side in 1(a). Further deformation generates an atomically sharp tip formed by 7 atomic layers in 1(c); the arrow indicates the formation of a twin defect at the 5th atomic layer (counting from the tip); after rupture 1(f), the twin defect is annihilated and the tip reorganizes itself to form a truncated pyramid. See supplementary material in [23].

From Fig. 1 we can also clearly observe the presence of a twin defect. On the experimental image it can be recognized by the angle present on the pyramid facets. Above the twin, the facets of the tip are a (111) plane on the left and a (100) on the right; below the twin they are a (111) plane on the right and a (100) on the left (see Fig. 2). We consider it as a twin in the sense that we observe an *ABCBA* arrangement, 5 planes stacking from the pyramidal bottom, where *C* is the mirror plane: \overleftarrow{ABCBA} [24]. Moreover looking closely at the tip, the last plane must be considered, in a strict sense, a stacking fault. However, this plane contains a single atom at the only possible configuration, seated at the center of a triangle arrangement; thus, we will not consider this as a defective structure.

One very important result is that during the NC formation no twin was observed very close to the tip. It has only been observed at the 4th layer [Fig. 1(d)] and at the 5th layer [Fig. 1(c)]. These results raise the important question whether this represents the transition size between the macroscopic plasticity mechanism and the nanometric scale where extended defects cannot be sustained anywhere [1]. In order to better address this question, we have analyzed the energetics associated with this defect formation. We have calculated the structure relaxation and the total energy of the structures shown in Figs. 3(a)–3(e). As the experimentally observed tip (Fig. 1) has seven layers, we have investigated all five possible positions for the twin defect, as shown in Fig. 3.

In order to model the pyramidal Pt tip based on our experimental data, we should consider that the HRTEM images provide a bidimensional projection of the atomic arrangements, but three-dimensional ones are needed to build input models for the calculations. The apex morphology is determined by the crystal faceting [12], which can easily be obtained using the Wulff construction rules [25].

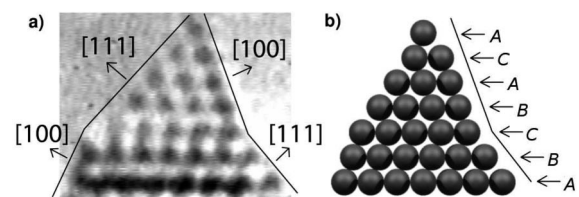


FIG. 2. (a) NC with a twin defect formed in its fifth layer counting from the top. (b) Schematic drawing of the tip in (a) showing the usual *ABC* notation for the fcc packing.

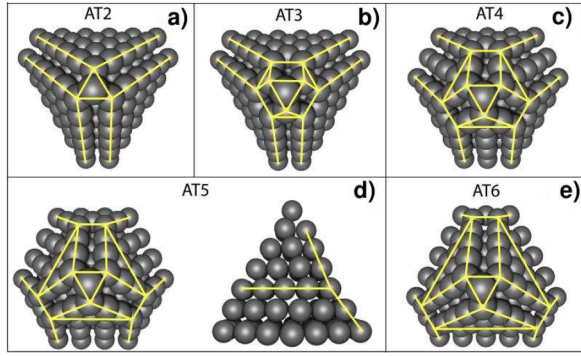


FIG. 3 (color online). Schematic drawing of possible atomic arrangement of twinned [111] Pt NCs. The schemes in (a)–(e) are organized as a function of the twin height position at the apex, second, third, fourth, fifth, and sixth layer, respectively. Lines indicate the atomic layer and the facet borders.

For the Pt structures in our case (Fig. 1) only (111) and (100) facets needed to be considered. However, additional factors must be taken into account in order to build an atomically sharp [111] tip. For example, the atom at the extreme of the tip is located at the center of a regular triangle (second layer), which by itself is located over a hexagonal structure [third layer, Fig. 3(a)]. As described above, although in this configuration the atom that finishes the tip is not in the expected crystallographic position, this is the unique way to construct the sharp pyramid. The triangular shape of the second layer fixes the apex [100] facet width to be two-atom row in size [Fig. 3(a), named AT2 apex]. To generate the twinned apexes, we must consider two crystalline domains: a base and a tip. A twin can also be seen as a 60° rotation of one of the domains along the tip axis; in this way, the (111) [or (100)] facets of the tip become (100) [or (111)] facets at the base (see Figs. 2 and 3). Although the domains are rotated, they must have exactly the same cross section at the twin. Briefly, the faceting pattern is determined by two geometrical constraints: (a) an atomically sharp apex imposing that the tip domain must be identical to the equivalent region of the AT2 apex; (b) the twin position, because the tip (100) [or (111)] facet width at the twin position will determine the width of the (111) [or (100)] facet at the base. As a consequence, these apexes will not always follow rigorously the Wulff surface balance, and also the total number of atoms in the tips will not be constant (see Table I).

Based on the procedure discussed above, we generated the 3D structures for the calculations. The initial Pt atomic positions followed a geometrically (or twinned) Pt lattice as schematically shown in Fig. 3, and then we have carried out geometrical optimizations. In Table I we present the relative energy formation: $E_{\text{struc}} - NE_a$, where E_{struc} is the energy of the configuration, N is the number of the atoms in the structure, and E_a the energy of one isolated atom. The results are relative to the lowest energy configuration (AT4).

These results can be explained in terms of faceting and stress release energy generated by the twin defect [1,25]. AT4 is the favored configuration because it allows, at the same time, a one-atom tip and an optimized base surface faceting [Fig. 3(c)]. Considering the GGA energy estimation, moving the defect one or two layers up (AT3 and AT2, respectively) costs a large amount of energy (40.94 and 40.69 eV, respectively). These structures present imperfect faceting, but the structural instability comes mainly from the loss of 6 atoms. In contrast, moving the defect one layer down (AT5) changes the structural energy by 0.84 eV. However, moving one layer further (AT6) requires a large amount of energy (28.89 eV), but considerably less than in the AT2 and AT3 cases. Also, the transition from AT5 to AT6 involves only the loss of 3 atoms. We should remark that the same conclusion can be obtained by a similar analysis done with LDA values (see Table I).

The AT5 apex represents the first available structure to absorb accumulated stress; this is in excellent agreement with our time resolved HRTEM observations which show that AT5 [Fig. 1(d)] is formed much before the NC thinning and rupture. As for the possible structural transition from AT4 to AT5 apexes, it is important to notice that we are dealing with very small systems with a large surface to volume ratio. The twin can be considered as a rotation between two configurations; this is certainly a very low cost process and probably with a low energy barrier for the size of the structures considered here, as described in the quasimelting of small Au clusters [26]. This interpretation can be better evidenced by the video in the supplementary material [23].

In order to verify whether the obtained results for Pt could be extrapolated to other metals, we repeated the calculations for Au and Ag, the most commonly used metals in NCs. As we observed that LDA and GGA produced consistent results, we have limited our calculation to

TABLE I. DFT formation energy estimated for twinned Pt, Ag, and Au NCs, with relation to the AT4 tip (see Fig. 3).

Twin Position (n)	Number of atoms	Pt (eV) (GGA)	Pt (eV) (LDA)	Ag (eV) (LDA)	Au (eV) (LDA)
2(AT2)	99	40.69	46.67	32.06	34.49
3(AT3)	99	40.94	47.02	32.20	34.59
4(AT4)	105	0.00	0.00	0.00	0.00
5(AT5)	105	0.84	1.35	0.51	0.36
6(AT6)	102	28.89	26.53	17.90	18.99

LDA ones for these cases due to GGA high computational cost. The results are displayed in Table I and the conclusions are similar, suggesting that these are general features of face centered cubic (fcc) metallic NCs. However, it must be noted that generated Pt twins can be blocked at room temperature due to a high energy barrier [27,28], much higher than thermal energy at room temperature. So, calculations neglecting temperature effects, such as the one presented here, can be considered a reasonable description of room temperature Pt NC experiments. On the other side, the comparison cannot be extended to Ag and Au NCs, because energy barriers are much lower [27,28]. Also, the lower barriers can account for the HRTEM results, which show that defects are quickly annihilated in Ag/Au NCs at room temperature for our time limit image acquisition of 30 frames per second [12,29]. But, it must be expected that the predicted Ag or Au size limit for twin defect formation should be observed in low temperature experiments.

In summary, we have shown that the elongation of Pt NCs induces the formation of twins located a few planes away from the apex, where the atomic arrangement of the atomically sharp Pt pyramid remains close to the ideal one. This means that it is possible to produce NC with a well defined structure. Many models in molecular electronics have assumed defect-free pyramidal NC as leads, which has been an object of criticism as being unrealistic. Our results showed that this is, in fact, a reasonable approximation. On the other hand, an extended defect will always be present beyond the fourth atomic plane counting from the tip and will work as a scattering plane. Thus, it is expected that full electron transmission coefficients are no longer possible, at least for Pt NCs. These aspects should be taken into account when modeling the typical two point electrical measurement on molecular electronic devices. Similar results were also obtained for Au and Ag, suggesting that this is a general behavior of fcc metals. Nevertheless, they should be observed only at lower temperatures (few Kelvin). The twin planes with areas approximately corresponding to the fourth or fifth atomic planes of the Pt pyramid may be considered as a lower size limit for defect generation.

This work was supported by IN/MCT, THEO-NANO, NANOMAT, LNLS, CNPq, and FAPESP. The authors thank P.C. Silva and J. Bettini for sample preparation and data treatment assistance.

*varlei@ifi.unicamp.br

- [1] U. Landman, W.D. Luedtke, N.A. Burnham, and R.J. Colton, *Science* **248**, 454 (1990).
- [2] R.M. Metzger and M.P. Cava, *Molecular Electronics: Science and Technology* (Annals of New York Academy of Sciences, New York, 1998), pp. 95–115.
- [3] C.P. Collier, E.W. Wong, M. Belohradský, F.M. Raymo, J.F. Stoddart, P.J. Kuekes, R.S. Williams, and J.R. Heath, *Science* **285**, 391 (1999).
- [4] J. Chen, M.A. Reed, A.M. Rawlett, and J.M. Tour, *Science* **286**, 1550 (1999).
- [5] M.A. Reed, C. Zhou, C.J. Muller, T.P. Burgin, and J.M. Tour, *Science* **278**, 252 (1997).
- [6] H.B. Akkerman, P.W.M. Blom, D.M. de Leeuw, and B. de Boer, *Nature (London)* **441**, 69 (2006).
- [7] J. Repp, G. Meyer, S. Paavilainen, F.E. Olsson, and M. Persson, *Science* **312**, 1196 (2006).
- [8] S.-H. Ke, H.U. Baranger, and W. Yang, *J. Chem. Phys.* **123**, 114701 (2005).
- [9] N. Agrait, A.L. Yeyati, and J.M. van Ruitenbeek, *Phys. Rep.* **377**, 81 (2003).
- [10] A. Hasmy, A.J. Pérez-Jiménez, J.J. Palacios, P. García-Mochales, J.L. Costa-Krämer, M. Díaz, E. Medina, and P.A. Serena, *Phys. Rev. B* **72**, 245405 (2005).
- [11] R.H.M. Smit, Y. Noat, C. Untiedt, N.D. Lang, M.C. van Hemert, and J.M. van Ruitenbeek, *Nature (London)* **419**, 906 (2002).
- [12] V. Rodrigues, T. Fuhrer, and D. Ugarte, *Phys. Rev. Lett.* **85**, 4124 (2000).
- [13] G. Rubio, N. Agrait, and S. Vieira, *Phys. Rev. Lett.* **76**, 2302 (1996).
- [14] G. Rubio-Bollinger, S.R. Bahn, N. Agrait, K.W. Jacobsen, and S. Vieira, *Phys. Rev. Lett.* **87**, 026101 (2001).
- [15] G.M. Dalpian and J.R. Chelikowsky, *Phys. Rev. Lett.* **96**, 226802 (2006).
- [16] S.C. Erwin, L. Zu, M.I. Haftel, A.L. Efros, T.A. Kennedy, and D.J. Norris, *Nature (London)* **436**, 91 (2005).
- [17] J.M. Soler, E. Artacho, J.D. Gale, A. García, J. Junquera, P. Ordejón, and D. Sánchez-Portal, *J. Phys. Condens. Matter* **14**, 2745 (2002); see also <http://www.uam.es/siesta>.
- [18] Y. Kondo and K. Takayanagi, *Phys. Rev. Lett.* **79**, 3455 (1997).
- [19] E.M. Fernández, J.M. Soler, and L.C. Balbás, *Phys. Rev. B* **73**, 235433 (2006).
- [20] N. Troullier and J.L. Martins, *Phys. Rev. B* **43**, 1993 (1991).
- [21] J.P. Perdew, K. Burke, and M. Ernzerhof, *Phys. Rev. Lett.* **77**, 3865 (1996).
- [22] F. Cleri and V. Rosato, *Phys. Rev. B* **48**, 22 (1993).
- [23] See EPAPS document No. E-PRLTAO-99-016750 for a video showing the elongation and rupture of a Pt NC under tensile stress with a minor shear component. The lower apex is well aligned with the HRTEM beam, thus providing atomic and time resolved images of a pyramidal tip contact. Its axis is along the [111] crystalline direction and, just before rupture, it ends with only one atom. For more information on EPAPS, see <http://www.aip.org/pubservs/epaps.html>.
- [24] N.W. Ashcroft and N.D. Mermin, *Solid State Physics* (Saunders College Publishing, Philadelphia, 1976), ISBN .
- [25] L.D. Marks, *Rep. Prog. Phys.* **57**, 603 (1994).
- [26] W. Krakow, M. José-Yacamán, and J.L. Aragón, *Phys. Rev. B* **49**, 10591 (1994).
- [27] M.J. Mehl, D.A. Papaconstantopoulos, N. Kioussis, and M. Herbranson, *Phys. Rev. B* **61**, 4894 (2000).
- [28] X. Wei, J. Zhang, and K. Xu, *Appl. Surf. Sci.* **253**, 4307 (2007).
- [29] V. Rodrigues, J. Bettini, A.R. Rocha, L.G.C. Rego, and D. Ugarte, *Phys. Rev. B* **65**, 153402 (2002).